Discharge Resistant Nano-coatings

Jing Xia[1,2], Zhengyu Li[1,2,3], Shamima Nasreen[1,2], JoAnne Ronzello[1,2], Henry Teng[4], Linda Jacobs[4] and Yang Cao[1,2,3]

[1] NSF Industrial University Collaborative Research Center on High Voltage/Temperature Materials and Structures
[2] Electrical Insulation Research Center, Institute of Materials Science, University of Connecticut
97 N. Eagleville Road, Unit 3136, Storrs, CT 06269 USA
[3] Electrical and Computer Engineering, University of Connecticut
371 Fairfield Way, U-4157, Storrs, CT 06269 USA
[4] ABB, 41 Woodford Ave, Plainville, CT 06062 USA

Abstract- **Nano-laminate coatings with highly ordered and oriented nanostructures based on Organically Modified Montmorillonite (o-MMT) were formed via co-assembling with polymer binders and applied by using various coating methods including spray coating, dip coating and blade cast coating for making films/coatings with enhanced dielectric and electrical discharge resistance. Dielectric properties of the nanoclay coatings along with their nanostructure characterization were studied for the coating processing optimization. The DC breakdown strength test and small-angle x-ray diffraction results consistently indicated that dip coated samples led to the most highly oriented nano-laminated structure with the highest breakdown strength. Corona endurance test was also performed on dip coated MMT nano-composite materials in comparison with other commercial available discharge resistant film. A remarkable enhancement was observed for nano-laminate coating, which indicated that this new nano-composite material has potential to be a processable and cost-effective dielectric material for many applications where discharge resistance device/structure/materials are needed.**

Keyword- *Montmorillonite (MMT), nano coating, discharge resistance, breakdown strength, XRD*

I. Introduction

Electric arc involves extremely high temperature, excessive heat generation, toxic mass release, and represents one of the most severe thermal plasma energy discharges that raise critical safety concerns. Considering the hazards and risks due to arc flashing and arc interruption, the development of high-performance discharge resistant dielectrics is imperative for a broad range of electrical power apparatus and applications. Preferably, such discharge resistant dielectrics shall be applicable in the form of coatings onto conformal structures or surfaces.

Traditionally, electrical discharge resistant materials have been developed based on mica, the applications of which dated back to 1940s as tape and much earlier as splits. As of today, micaceous insulation has been predominantly used in electrical rotating machines ca. power generators and electric motors due its superior discharge resistance. The best electrical discharge resistance properties in mica are retained in the form as mica tape insulation, i.e., mica paper laminated with glass-fabric backing via epoxy binder. This form of application delivers one of the best electrical discharge resistances among all major types of electrical insulations. However, its restricted forms of application as either taping or laminate limit significantly the applicability of micaceous insulation. For instance, many modern applications require conformal coating or injection molded insulation with superior discharge resistance. Besides, after decades of evolution, this mica paper/glass-fabric laminate can no longer meet the requirements of modern power generation, conversion and protection devices/apparatus. For instance, high layer thickness of mica insulation system behaves as a barrier of thermal transportation [1].

To achieve further improvement over current technology, researchers are focusing on the development of composite materials containing nano-sized particles with mica-like structures. Ideally, composite material with well dispersed discharge resistant nano-size fillers should lead to a better long-term lifetime against discharge erosion as well as the enhancement of power density or downsizing due to improvement of thermal transportation of thinner layer thickness [1-3]. Moreover, it is highly desirable that these new materials/structures can be applied in free form or via additive manufacturing processes.

Montmorillonite (MMT) nanoclay, as an important inorganic nanoclay that belongs to the same crystalline structure family of mica, is composed of joint silica and alumina sheets with a high aspect ratio (length/width) of 1 nm in thickness over several hundred nm in lateral dimensions. The chemical composition of MMT is described by general formula of $M^{+}_{y}(Al_{2-y}Mg_{y})(Si_{4})O_{10}\cdot nH_{2}O$ [4]. The particle size of MMT in its delivery form is micro-scaled aggregates. However, it is feasible to exfoliate MMT aggregates into nano-scale platelets which then can be co-self-assembled with polymer binders into a tough, transparent and flexible film. For better intercalation and possibly exfoliation in the non-polar polymer matrix, MMT could be organically modified to obtain the optimized polarity [5-7]. Previous research and studies have already proven that the clay/polymer nanolaminate films have numerous advantages that could bring remarkable improvements in physical or chemical properties, such as flame resistance, optical clarity, barrier properties as well as dielectric properties [5, 8, 9]. In this research, MMT particles were completely exfoliated down to nano-scale 2-D sheets and combined with polymer binders to form highly oriented laminating film samples through the self-assembling process in non-polar solvent. Nanostructure observation as well as dielectric properties study were performed to further examine the improvement based on the applied nano-coatings.

978-1-5386-6192-5/18/$31.00 ©2018 IEEE

II. Samples and Experimental Setup

A. Material Preparation

Organic modified MMT clay (Cloisite 20A, BYK) was exfoliated and co-assembled with the polymer binder into nanolaminate coatings or free-standing films. Oven-dried MMT was dispersed in a mixture solvent by magnetic stirrer followed by ultrasonication with a probe type ultrasonicator (Sonic Dismembrator Ultrasonic Processor, Model No. 705) to exfoliate the MMT aggregates into nano-scaled single layer [10]. Second sonication was applied after mixing with the binder at a weight ratio of 20%:80%.

Nanolaminate coatings/films were formed by three different coating process, namely spray coating, dip coating and blade casting. Multiple layers were applied to build up desirable thickness to form free-standing films. Samples were dried at 80°C for 3 hours to remove residual solvent and stress.

B. Experimental Setup

The coatings were characterized for microstructural analysis by using small-angle X-ray diffraction and Scanning Electron Microscope (SEM) and for dielectric properties by using DC breakdown, corona discharge endurance and dry band tracking tests.

Small-angle X-ray diffraction (SAXRD) measurement was performed using a Cu Ka (λ=1.54056Å) radiation generated by a Bruker system. Samples were mounted on a single crystal silicon coated stage to avoid reflection noise.

The DC breakdown test was performed using a DC high voltage power supplier (Stanford Research, PS375) with a constant ramping rate of 300V/s at room temperature (~ 25°C). The polymer film samples were sandwiched in between two metallized biaxially oriented polypropylene (BOPP) film electrodes. The active test area of 1.4 ×1.4 cm^2 was set with a 75 µm polyimide (Kapton® HN) mask. With the application of high voltage, an electrostatic force at MPa level is induced between the high voltage electrode and the ground electrode, which will ensure good contacts between sample and the electrodes and eliminate any possible air gaps or air bubbles [10].

The corona endurance test was performed with three sets of samples including 50 µm blank polyimide film (PI 1), 50 µm blank PI 1 with 2 µm nano-composite coating and 50 µm discharge resistant polyimide film (PI 2). A cylindrical SS electrode of 6.35 mm-diameter with a 1 mm round edge was used as the upper HV electrode. Another metal plate with diameter of 25.4 mm was used as the bottom grounding electrode. Samples were cut into 50 × 50 mm^2 squares to avoid surface flashover. Ten pairs of such electrode/sample configurations were installed on a test rack for one type of sample. The high voltage electrode was made in contact with the sample by the natural force of gravitation. All samples were dried under vacuum for more than 24 hours prior to testing and the corona endurance test was conducted in a chamber with controlled air flow.

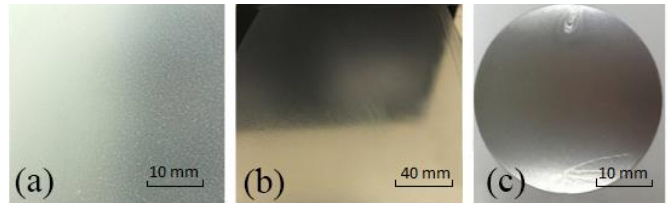

Fig. 1. Appearance of nanocoating films. (a) Free standing Spray coated film; (b) Blade casted film on ferrotype plate; (c) Dip coated film on SS shim stock.

III. Results and Discussion

A. Small-angle X-ray Diffraction (SAXRD)

The 2-D diffraction patterns for nanoclay coatings prepared by various methods of coating were analyzed by SAXRD to quantify their nano-lamination structure. Interlayer spacing and degree of orientation were calculated from the first order diffraction peaks observed.

The first order diffraction peaks of films prepared by spraying, dipping and blade casting were found at 2.70°, 2.56° and 2.61°, respectively, while the corresponding second order diffraction peaks were found at 5.40°, 5.12° and 5.22° with the same intervals, as shown in Fig. 2. Interlayer spacing could be calculated through Bragg's Law as

$$d = \frac{n\lambda}{2sin\theta} \quad (1)$$

where d is the interlayer spacing of MMT/binder nano-lamination and λ is X-ray wavelength. Interlayer spacing distance was calculated as 3.27 nm, 3.45 nm and 3.38 nm for spray coating, dip coating and blade cast coating, respectively. The exfoliated MMT nanosheet has a thickness of 1nm [11]. Thus, the thicknesses of intercalation spacer/binder for three

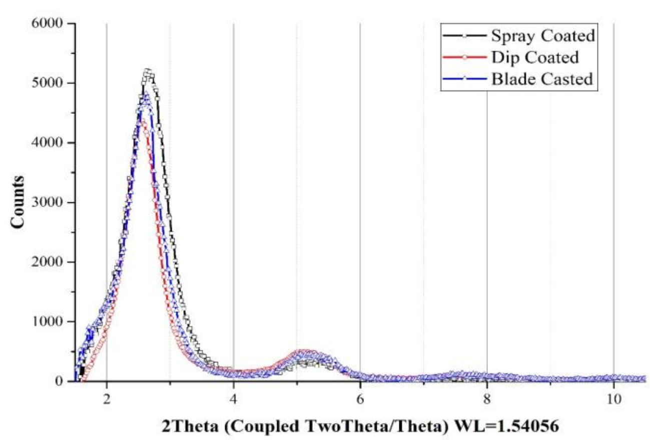

Fig. 2. SAXRD data for nanoclay coatings by spray/dip/blade cast processes.

coatings were estimated to be 2.27 nm, 2.45 nm and 2.38 nm, respective.

Half-width of SAXRD peak corresponds to the degree of orientation of lamination structure and smaller half-width represents higher degree of orientation. The estimated half widths of these three methods of coating were 0.74, 0.57 and 0.62, respectively. With the smallest half-width, dip coated

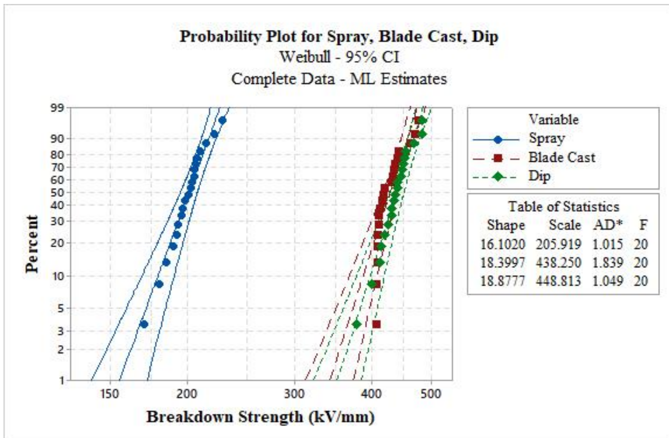

Fig. 3. Weibull distribution plot of dc breakdown strength with 95% confidence range.

samples appear to be with the highest degree of oriented lamination structure, making it an attractive method for producing samples to be tested against commercial materials.

B. DC Dielectric Breakdown Test

To evaluate the dielectric breakdown strength of the coated films, Weibull parameter estimation, a powerful tool in failure analysis, was employed to analyze the breakdown test results. The probability density function (PDF) is expressed as

$$f(x;\alpha,\beta) = \begin{cases} \frac{\beta}{\alpha}\left(\frac{x}{\alpha}\right)^{\beta-1} e^{-\left(\frac{x}{\alpha}\right)^{\beta}}, & x \geq 0 \\ 0, & x < 0 \end{cases} \quad (2)$$

where $\beta > 0$ is the shape parameter and $\alpha > 0$ is the scale parameter. Weibull characteristic breakdown strength is reported with the accumulative failure probability of 63.2%. Coating thickness was measured multiple times near the site of breakdown and the average was used to determine the breakdown strength. Breakdown data were analyzed and plotted in Weibull distribution as shown in Fig. 3. The breakdown strengths are 206 kV/mm for spray coated film, 440 kV/mm for blade cast coating, and 449 kV/mm for dip coated coating, respectively. The dip coating and blade cast yield coatings with two best and similar dielectric breakdown strength of ~440-450 kV/mm, with the one by dip being slightly better. The high breakdown strength is generally higher than some traditional discharge resistant materials such as micaceous insulation [2]. The spray coated film has a relatively lower breakdown strength. However, the spray coating process has the advantage of producing with high through-put coatings in free standing in large thickness. Also, the spray coating can be applied to high conformal structures or surfaces.

TABLE I
COMPARISONS OF SAXRD DATA AND DC BREAKDOWN STRENGTH RESULTS FOR VARIOUS COATING PROCESSES

Sample	D-spacing at 1st peak (°)	Half-width at 1st peak (°)	Breakdown Strength (kV/mm)
Spray	2.70	0.74	205.9
Dip	2.56	0.57	448.8
Blade Cast	2.61	0.62	440.7

The variation of dielectric breakdown strength of nanoclay coatings prepared in this study by different methods of application appears to correlate well with the ordering and degree of orientation of their corresponding nanolamination structures, as suggested by the D-spacing and half-width data at the first order peak summarized in Table I. It is interesting to observe that the D-spacing and half-width value for dip and blade cast coatings are in similarly low and tight values indicating better lamination ordering and degree of orientation, which translate to higher DC breakdown strength, in comparison with the spray coated film. Furthermore, such correlation implies the plausible barrier properties imparted from highly oriented MMT nanolamination in through thickness direction to enhance the DC breakdown strength.

C. Corona Resistance Test

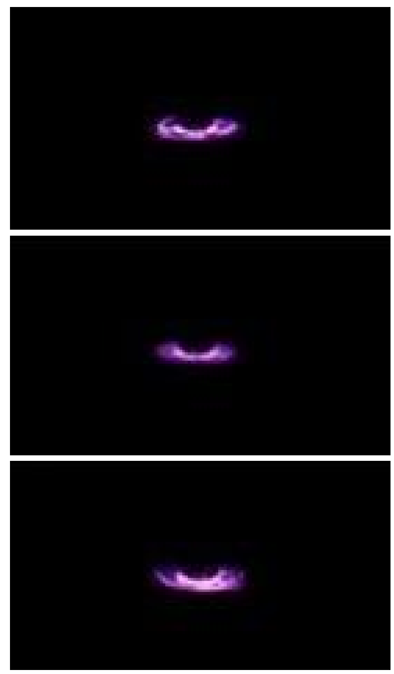

Fig. 4. Corona discharge patterns on the surface of blank PI 1 film (top), nanoclay coated PI 1 film (middle), and PI 2 film (bottom) under 100kV/mm.

Discharge resistance performance of the dip and blade cast coated nanoclay coating films was evaluated along with the spray coated film for potential alternatives of discharge resistant dielectrics used in high voltage/high current systems. The corona endurance test was performed in accordance with IEC-60343 standard in rod to plane electrode configuration, where corona discharges are initiated from the edge of the electrode with the local electric field exceeding the corona discharge inceptions. Electric fields of 46 kV/mm and 100 kV/mm both in power frequency were applied to the samples under test, respectively. Appearance of the corona on these films under 100kV/mm was captured as shown in Fig. 4. A bright corona appeared around the high voltage electrode on the

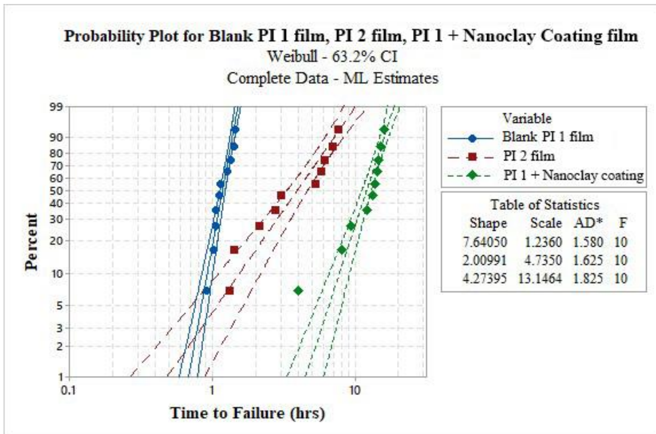

Fig. 5. Weibull distribution plot of corona endurance test time to failure with possibility of 63.2%.

non-discharge-resistant polyimide film (blank PI 1), generated and developed periodically into sparks and streamers along the surface. For the commercial discharge resistant material, PI 2 film, it was seen with nearly same level of corona discharge intensity, along with sparks as well as streamers on the surface. However, for the nano-coated film, there was a significantly reduction in the brightness of the corona. In addition, the number and frequency of sparks and electric streamers were also largely decreased. In comparison with PI 2, the discharge pattern around electrodes on nanoclay coated PI was very uniform and stable (spatially and temporally) and rarely developed into highly branched streamers with high light intensity. This suppression of electrical discharge is attributed to the electrical barrier properties of nanolamination structure as well as its anisotropic electrical conductivities which act collectively as barriers with grading features.

To better quantify the discharge resistance, time to failure of each sample was recorded and analyzed using Weibull statistical analysis with results shown in Fig. 5. Under 46 kV/mm, blank PI 1 fails at roughly 10 hours, while other two sets of samples lasted over 66 hours. As for under 100 kV/mm, blank PI 1 films have a Weibull characteristic failure time of 1.2 hours and PI 2 films have a failure time of 4.2 hours with large variations. In comparison, nanoclay coated films possess a much-improved average time to failure of 11.9 hours, with longest survivor at 15.7 hours leading in all samples tested.

IV. Conclusions

Nano-laminate coatings with highly ordered and oriented nanostructures based on o-MMT were formed via co-assembling with polymer binders and applied by three coating processing methods i.e., spray coating, dip coating and blade cast coating. Nanostructure characterization was performed to analyze the degree of orientation of the inorganic fillers in the polymer matrix. As one of the most significant dielectric properties, DC breakdown strength was also investigated, which correlates well with the structure analysis. The results suggest that nano-scale polymer intercalated clay laminates with high degree of orientation could behave as an electrical barrier with remarkably improved dielectric properties. Corona endurance test was performed on nanoclay coated materials together with other commercial available discharge resistant materials. Nanolaminate coatings exhibit superior discharge resistance to benchmarking materials. The impressive enhancement of discharge endurance as well as highly enhanced DC breakdown strength indicate clearly that with further optimization these new nanolaminate materials will find broad range of applications in high voltage power system and apparatus.

Acknowledgment

The authors thank Hiep Nguyen and Zongze Li for assistance with the experiment setup and analysis. We thank all other members at the Electrical Insulation Research Center of the University of Connecticut for their support and suggestions regarding this research.

References

[1] M. Kaufhold, K. Schafer, K. Bauer, A. Bethge and J. Risse, “Interface phenomena in stator winding insulation-challenges in design, diagnosis, and service experience,” IEEE Electr. Insul. Mag., vol. 18, pp. 27-36, 2002.

[2] R. Vogelsang, T. Farr and K. Frohlich, “The effect of barriers on electrical tree propagation in composite insulation materials,” IEEE Trans. Electr. Insul. Mag., vol. 13, pp. 373-382, 2006.

[3] Y. Cao, Patricia C. Irwin and Karim Younsi, “The Future of Nanodielectrics in the Electrical Power Industry”, IEEE Trans. Dielec. Insul., Vol. 11, pp.797-807, 2004.

[4] R.A. Vaia, B.B. Sauer, O.K. Tse and E. P. Giannelis, “Relaxations of confined chains in polymer nanocomposites: glass transition properties of poly (ethylene oxide) intercalated in montmorillonite,” Journal of Polymer Science Part B: Polymer Physics, vol. 35, pp. 59-67, 1997

[5] E. Dunkerley, H. Koerner, R.A. Vaia and D. Schmidt, “Structure and dynamic mechanical properties of highly oriented PS/clay nanolaminates over the entire composition range,” Polymer, vol. 52, pp. 1163-1171, 2011

[6] E. Dunkerley and D.F. Schmidt, “Understanding the Consequences of Intercalation Using Model Polymer Nanolaminates,” Macromolecules, vol. 48, pp. 7620-7630, 2015

[7] S.P. Fillery, H. Koerner, L. Drummy, E. Dunkerley, M. F. Durstock, D. F. Schmidt, and R. A. Vaia, “Nanolaminates: Increasing Dielectric Breakdown Strength of Composites,” ACS applied materials & interfaces, vol. 4, pp. 1388-1396, 2012

[8] S. Pavlidou and C.D. Papaspyrides, “A review on polymer–layered silicate nanocomposites,” Progress in polymer science, vol. 33, pp. 1119-1198, 2008

[9] P. Podsiadlo, A. K. Kaushik, E. M. Arruda, A. M. Waas, B.S. Shim, J. Xu and H. Nandivada et al., “Ultrastrong and stiff layered polymer nanocomposites,” Science, vol. 318, pp. 80-83, 2007

[10] M. Ren, J. Liu, L. Sun and Y. Cao, “Enhancing Dielectric Property of Polymer Films with Nanoclay Coatings,” IEEE Annual Conference on Electrical Insulation and Dielectric Phenomena, pp. 651-654, 2016.

[11] C. Wan, X. Qiao, Y. Zhang and Y. Zhang, “Effect of different clay treatment on morphology and mechanical properties of PVC-clay nanocomposites,” Polymer Testing, vol. 22, pp. 453-461, 2003